Contraction speed of the actomyosin cytoskeleton in the absence of the cell membrane†

Gustavo R. Plaza*[ab] and Taro Q. P. Uyeda[cd]

The contraction of the actomyosin cytoskeleton, which is produced by the sliding of myosin II along actin filaments, drives important cellular activities such as cytokinesis and cell migration. To explain the contraction velocities observed in such physiological processes, we have studied the contraction of intact cytoskeletons of *Dictyostelium discoideum* cells after removing the plasma membrane using Triton X-100. The technique developed in this work allows for the quantitative measurement of contraction rates of individual cytoskeletons. The relationship of the contraction rates with forces was analyzed using three different myosins with different *in vitro* sliding velocities. The cytoskeletons containing these myosins were always contractile and the contraction rate was correlated with the sliding velocity of the myosins. However, the values of the contraction rate were two to three orders of magnitude slower than expected from the *in vitro* sliding velocities of the myosins, presumably due to internal and external resistive forces. The contraction process also depended on actin cross-linking proteins. The lack of α-actinin increased the contraction rate 2-fold and reduced the capacity of the cytoskeleton to retain internal materials, while the lack of filamin resulted in the ATP-dependent disruption of the cytoskeleton. Interestingly, the myosin-dependent contraction rate of intact contractile rings is also reportedly much slower than the *in vitro* sliding velocity of myosin, and is similar to the contraction rates of cytoskeletons (different by only 2–3 fold), suggesting that the contraction of intact cells and cytoskeletons is limited by common mechanisms.

Introduction

In eukaryotic cells, the cytoskeleton provides scaffolds for intracellular organization, internal cargo transportation, mechano-sensitivity, rigidity and strength, and directs dynamic changes during crucial processes such as cell migration and division.[1,2] The actin–myosin system makes the cytoskeleton contractile, and it drives dynamic cytoskeletal reorganizations. Understanding its dynamic behavior and architecture is important to elucidate aspects such as the interaction with other cellular components and the response to external stimuli. In fact, the contractile behavior of the cytoskeleton is affected not only by biochemical signaling but also by internal and external forces and by osmotic pressure. The purpose of this study was to explain the physiological contraction speeds by studying the contraction of the cytoskeleton in the absence of the cell membrane, so that the cytoplasmic liquid can flow through the cell cortex and the physiological difference of pressure – osmotic pressure – is removed.

The cytoskeleton constitutes an example of a hierarchically organized system in which the rich behavior emerges from elementary interactions among components.[1] A chief constituent of the cytoskeleton is the network composed of actin filaments (F-actin) and filaments of myosin II (also called conventional myosin and referred to as simply myosin in the text). It is typically most dense in the cortical region of the cell, so that it is sometimes called actomyosin cortex. This system also contains regulatory proteins, which direct the nucleation, polymerization or depolymerization of actin filaments and, in the case of cross-linking proteins, connect neighboring actin filaments. Therefore, the whole arrangement of actin filaments and cross-linkers constitutes a continuous actin network, which in turn is directly or indirectly tethered to integral membrane proteins.[3–5] Myosin molecules are assembled into large bipolar filaments of tens to hundreds of myosin molecules with N-terminal heads in both extremes;[6,7] in *Dictyostelium discoideum*, each filament contains 10–20 myosin molecules.[8] The heads are molecular motors that hydrolyze ATP as fuel to actively generate forces and slide along actin filaments.[9,10] As a result, the

actomyosin cytoskeleton is a contractile network[11,12] which is an essential component in processes such as cell migration[13,14] or constriction of the contractile ring during cell division.[15–19]

In a contracting actomyosin cytoskeleton, there are two processes taking place simultaneously: sliding of myosin heads along actin filaments and remodeling of the actin filament network such as polymerization, depolymerization, rearrangement of cross-linking and bundling, and branching of actin filaments. Both processes are interrelated: on the one hand, sliding of myosin heads induces deformation in the actin network, causing different degrees of stretching and bending in the actin filaments,[20] and presumably detaches cross-linking proteins physically; on the other hand, stretching filaments alters their affinities for actin binding proteins, including enhanced affinity for the myosin II motor domain[21] and reduced affinity for cofilin.[22] Besides, the curvature of the filaments influences the formation of new branches.[23] During the contraction process, the forces introduced by myosin heads work on the cell cortex to deform it against resistive stresses.[24]

The detailed molecular architecture of the cytoskeleton and the characteristics of the changes in the actin network during the contraction process, on the length scale of tens of nanometers, remain an intriguing mystery. However, the dynamics of the whole system, on a length scale of micrometers or tens of micrometers, have been investigated in previous experimental works. These investigations followed two alternative strategies: a first group of works used living cells to study phenomena such as the formation of protrusions or blebs,[25–27] the contractile ring during cytokinesis[24,28,29] or the relationship between cell shape, actomyosin cortex and osmotic pressure.[1,30] These studies showed that the actomyosin cortex is an actively contracting network, which is tethered to the plasma membrane, and equilibrates osmotic pressure in the cytoplasm.[31] The cortex is a robust system, and myosin and actin can rapidly diffuse in the cytoplasm so that when a protrusion is produced in the membrane, new underlying cortex is rapidly assembled beneath the protruded membrane to recover equilibrium.[25] Besides, the system may be redistributed: actin and myosin molecules are recruited to take part in the contractile ring function during cytokinesis, in which myosin motors generate internal forces,[24,28,32] or to the sites of mechanical deformation by external forces.[33–35] A second group of studies examined the contraction of cytoplasmic extracts[11,12,36,37] or simplified model gels containing actin filaments, myosin motors and cross-linkers.[36,38–40] In these simpler reconstituted systems, contraction is achieved when the concentrations of actin, myosin and cross-linkers are within the appropriate range, the contraction speed being dependent on the concentrations.[36] Both in the case of the contractile ring during cytokinesis and in simplified reconstituted gels, the size of the system was observed to decay exponentially during the main part of the process.[24,36]

We studied the dynamics of contracting cytoskeletons from the cellular slime mold *Dictyostelium discoideum* cells obtained by removing the plasma membrane using Triton X-100 (ref. 11 and 12) and observed the process by microscopic imaging. This procedure allowed us to describe the process and measure the contraction rate of individual complete cytoskeletons, and compare the results with events such as blebbing or furrowing of the contractile ring during cytokinesis. Five cell lines were studied, each of them expressing myosins with different mechanical properties or lacking one of the two major actin cross-linking proteins. We found that myosin heads with a longer lever arm produce higher contraction rates, and that actin cross-linking proteins play a major role in the contraction process and maintain the integrity of the cytoskeleton. The results for substrates with different adhesiveness also show that the external resistive forces influence the contraction rate.

Results

The progression of contraction is described by the strain rate

In the actomyosin cortex, myosin is the molecular motor driving active contraction. It is required for the ATP-dependent contraction of *Dictyostelium* Triton cytoskeletons.[11,12] We verified that the cytoskeletons obtained from HS1 cells, not expressing myosin, did not contract upon the addition of ATP. The actomyosin cortex is linked to the plasma membrane and produces the cortical tension required to equilibrate osmotic pressure.[31] Therefore, removal or disruption of the membrane is necessary to allow contraction of the cytoskeleton. We solubilized the plasma membrane of *Dictyostelium* cells with 0.2% Triton X-100. 'Triton ghosts' produced in this way contain the actomyosin cytoskeleton, the nucleus and also debris of other organelles.[12,41] We used time-lapse fluorescence imaging to directly observe the cytoskeletons containing GFP–myosin. Apart from cells expressing GFP–wild type (wt) myosin, two additional strains of cells expressing GFP-fused mutant myosins were studied: a mutant myosin with an internal deletion that removes the regulatory light chain binding site, ΔRLCBS,[42] and a mutant lacking both light chain binding sites, ΔBLCBS.[43] During the movement of myosin heads along actin filaments, the light chain-binding domain within the motor domain rotates around an axis at the base of the neck region, like a lever. The length of the lever arm for the three myosins is 8.8, 5.8 and 1.8 nm for wt, ΔRLCBS and ΔBLCBS, respectively.[43] The observation of the contraction process was made possible by using substrates of either low adhesiveness (prepared using a poly-L-lysine aqueous solution of 0.0001% w/v) or high adhesiveness (0.0010% solution).

In the experiments, a first contraction was observed after the addition of the Triton solution, presumably due to the presence of endogenous ATP, and further contraction was made possible by the addition of ATP in the medium (the presence of NaN_3 in the buffer inhibits the endogenous production of ATP and, in specific experiments, we found that the initial contraction was negligible if the Triton solution was added after at least 10 minutes of incubation with NaN_3). Fig. 1 shows the progressive contraction of three cytoskeletons, which had not been treated with NaN_3 prior to the Triton treatment. After the addition of Triton X-100, the cytoskeletons underwent, at first, a small contraction, followed by a second larger contraction after the addition of ATP, until the maximum contraction was achieved. We verified that further addition of ATP did not produce additional contraction. Fig. 1b shows true strain,[44] calculated as

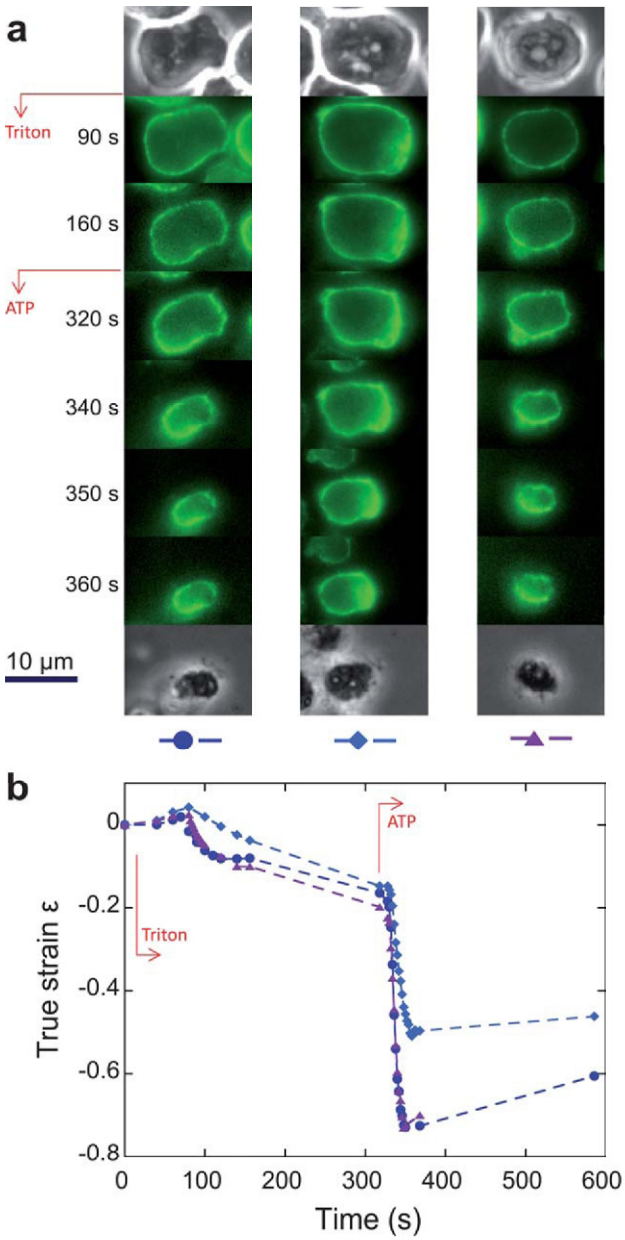

Fig. 1 Contraction process for three cytoskeletons with wt myosin on the low adhesiveness substrate (prepared using a solution of 0.0001% poly-L-lysine). The three cytoskeletons were imaged simultaneously. (a) Series of images showing the initial live cell (phase contrast microscopy), the cytoskeleton at different times during the contraction process (GFP–myosin observed by fluorescence microscopy, in green), and the final contracted Triton ghost (phase contrast microscopy). (b) True strain *vs.* time for the three cytoskeletons during the progression of contraction. The arrows show when Triton X-100 (0 s) and ATP were added (320 s).

$\varepsilon = \ln(L/L_0)$, with L the instant size and L_0 the initial size of the cell, *vs.* time. The contraction rate is defined as $r_c = -d\varepsilon/dt$. Estimation of the maximum contraction strain rate is obtained from the curve.

The time course of changes in the size of the actomyosin cortex has been previously studied by measuring the diameter of the contractile ring during cytokinesis of *Dictyostelium* cells.[24,45] Other works studied the contraction of reconstituted gels of actin, myosin II and α-actinin cross-linkers.[36] In both cases, the size of the system was found to follow an exponential decay during the main stage of the contraction process. Such an exponential decay takes place when the contraction strain rate r_c is constant: from its definition, the contraction rate can be written as $r_c = -(dL/dt)/L$ and, integrating this equation, the time course of changes in size L along time is given by the exponential function $L = L_0\exp(-r_c t)$. As shown in the following sections, most of the contraction produced in the cytoskeletons takes place during a short time interval, and we calculated the contraction strain rate achieved during that interval. We observed that the cytoskeletons remained contracted for over 24 h, after a reduction in GFP-content by diffusion, indicating that they had undergone plastic deformation.

In the initial conditions of the experiments (in the lysis buffer), the shape of the cytoskeletons was sensibly circular, with a mean circularity of 0.940 ± 0.008 [mean ± 95% confidence interval (CI), see Fig. S1†]. On average, the final circularity, 0.935 ± 0.007, was equal to the initial circularity (Fig. S1†).

Fig. 2a shows initial size *vs.* minimum (contracted) size for the cytoskeletons expressing one of the three GFP–myosins on one of the two substrates. The range of the initial size was broad, from 6.5 to 20 μm. The largest sizes were measured in cells with the mutant myosins, which suggests that these cells fail to divide more frequently than those expressing wt myosin, leading to multinucleation. The minimum size was always smaller than 8 μm, and up to ~12.5 μm of the initial size there was a positive correlation between minimum size and initial size. The maximum contraction, defined as the reduction in size divided by the initial size, is represented in Fig. 2b: since the minimum size was always in the range of 3 to 8 μm, the maximum percentage of contraction grew with the initial size. Cytoskeletons with wt myosin contracted by 44 ± 4% (mean ± 95% CI). Interestingly, ΔBLCBS and ΔRLCBS myosin cytoskeletons reached a similar maximum contraction to wt myosin (Fig. 2a), although at different strain rates.

Contraction rates: the contraction is faster for myosin with a longer neck domain

The contraction rates of the cells expressing three different myosins were computed from the strain *vs.* time curve. In the three cytoskeletons with wt myosin shown in Fig. 1b, the maximum contraction strain rates were reached between 335 and 345 s.

Fig. 2c shows the maximum contraction rate, as a function of the myosin type, for the two substrates with different adhesiveness (see ESI, Table S2†). The longer the lever arm was, *i.e.* the faster the sliding speed of unloaded myosin heads was (measured for actin filaments over myosin-coated surfaces *in vitro*), the higher the contraction strain rate was.[43] ΔBLCBS myosin showed similar rates on both substrates. However, the cytoskeletons with the other two types of myosin slowed down on the more adhesive substrate, suggesting that the adhesiveness of the substrate may introduce friction-like forces during the contraction process. Nonetheless, cytoskeletons on the weakly adhesive substrates appeared to experience little

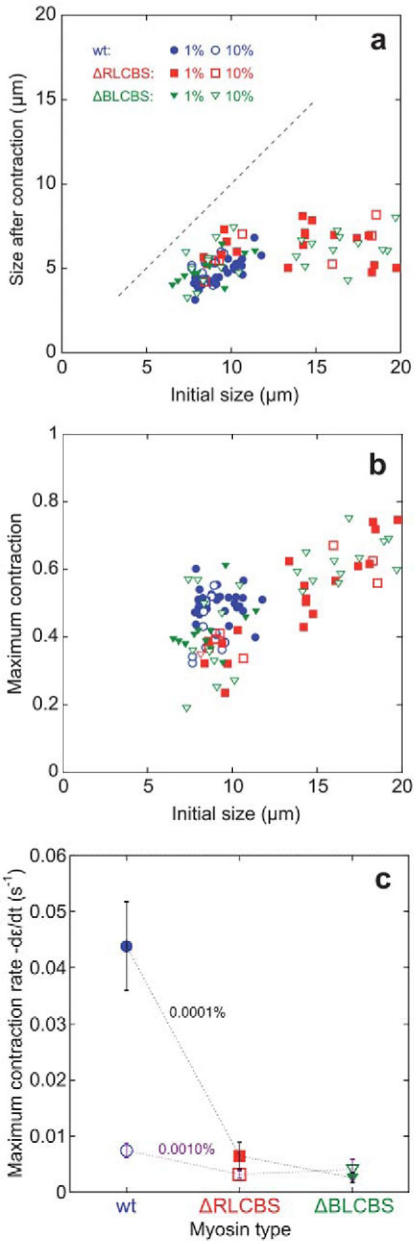

Fig. 2 Relationship between the sizes and strain rates of the cytoskeletons for the three different myosins and the two different substrates. (a) Size after contraction (*i.e.* minimum size) *vs.* initial size; it can be seen that there are no cytoskeletons with wt myosin with an initial size above 12.5 μm. (b) Maximum contraction *vs.* initial size; the contraction is defined from the minimum size L_{min} and the initial size L_0 as $(L_0 - L_{min})/L_0$. (c) Maximum contraction rates; the mean values are calculated for cytoskeletons with initial size less than 12.5 μm so that the range of the initial size is the same in all groups (the results are similar if all data are included; see ESI, Table S2†). Error bars indicate 95% CI.

friction, if at all, since most of the cytoskeletons drifted away during the experiments when we used substrates prepared by pretreatment with poly-L-lysine solutions below 0.0001%. As discussed below, the longer lever arm explains the higher sensitivity of wt myosin to the adhesiveness of the substrate.

For wt myosin, the maximum contraction rates were 0.044 ± 0.008 s^{-1} and 0.007 ± 0.001 s^{-1} (mean ± 95% CI) on the weakly and strongly adhesive substrates, respectively. The measured maximum contraction rate for cytoskeletons with wt myosin on the weakly adhesive substrate, ~0.04 s^{-1}, is similar to the rate measured in wt AX2 cells, as shown below. With this rate, a cytoskeleton needs around 15 s to contract to one half of its initial size (see ESI, Table S3†). This time is comparable to that obtained by Kuczmarski *et al.* (1991) using suspensions of Triton cytoskeletons, consistent with the idea that our weakly adhesive substrates did not impose appreciable load to the contraction.

The difference in myosin content is not a determinant of the contraction rate

The influence of the myosin content on the behavior of the cytoskeletons was analyzed, quantifying the content by mean fluorescence intensity. We found that the myosin content, within the range examined here, is neither related to the maximum contraction nor to the contraction rate. Fig. 3 illustrates this observation displaying the contraction rate *vs.* mean intensity for three groups of cytoskeletons imaged simultaneously, showing that the correlation is statistically insignificant (*P*-values of 0.11, 0.77, and 0.78 in these three examples).

The contractile behavior is substantially affected by cross-linking proteins

Several actin binding proteins are known to cross-link the actin filaments, with important roles in the actomyosin cortex. At least 11 genes for actin cross-linking proteins have been identified in the *Dictyostelium* genome.[46] We selected α-actinin and filamin, two of the most abundant cross-linking proteins in *Dictyostelium*, to analyze their influence on the contraction rate of the cytoskeletons. The functions of both proteins have been intensively studied in reconstituted actin networks[47,48] and in the *Dictyostelium* phenotype.[46,49–51] Therefore, the experiments were carried out with mutant *Dictyostelium* strains lacking α-actinin or the filamin gene, labeled respectively as α-actinin-null and filamin-null. These two null mutations in single highly conserved proteins have been reported to result in relatively minor phenotypes:[49,50] in the vegetative state, reduced growth rate under osmotic stress was observed in the α-actinin-null strain but no significant differences were found for the filamin-null strain. Instead, the filamin-null strain showed defective phototaxis of slugs during the development of fruiting bodies. In the experiments with these two mutant strains, we utilized weakly adhesive substrates.

Interestingly, α-actinin-null cytoskeletons on the weakly adhesive substrates presented the highest contraction rate measured in this work: 0.096 ± 0.033 s^{-1} (mean ± 95% CI), double the contraction rate of wt (AX2 cells) cytoskeletons: 0.042 ± 0.016 s^{-1}. In addition, α-actinin-null cytoskeletons reached the minimum contracted size, 3.5 ± 0.7 μm (contraction 63 ± 4%), significantly smaller ($P = 0.029$) than the wt cytoskeletons, 4.8 ± 0.9 μm (52 ± 5%). Accordingly, α-actinin-null cytoskeletons reached in some cases very small sizes, expelling most of the organelles and the nuclear DNA, as shown in Fig. 4b and c.

Filamin-null cytoskeletons showed a very different behaviour. In this case, most of the cytoskeletons quickly lost their integrity after the addition of ATP: GFP–myosin was dispersed

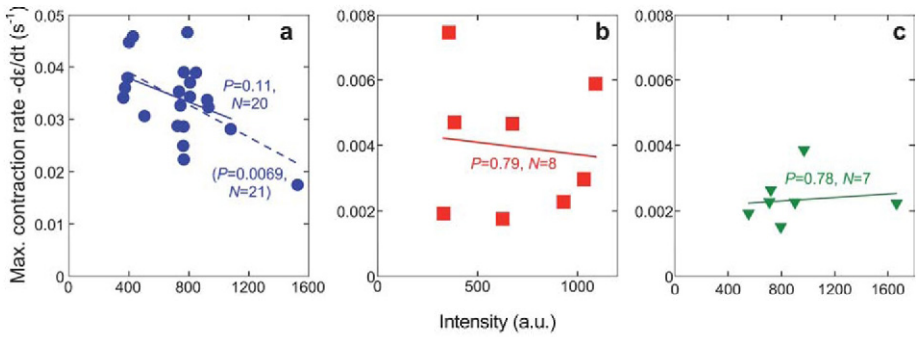

Fig. 3 Relationship between contraction strain rate and myosin content. The content of myosin is quantified by the mean fluorescence intensity in the cytoskeleton. The figure shows three groups of cells imaged simultaneously during the progression of contraction on the low adhesiveness substrate for (a) wt, (b) ΔRLCBS and (c) ΔBLCBS myosins. Each graph shows the line obtained by linear regression and the *P*-value that indicates the statistical significance (*t*-test) for the null hypothesis of slope equals zero. Panel (a) also shows the line obtained after removing the outlier point (broken line).

in the medium, although part of the actin cortex remained after myosin was lost. An example is shown in Fig. 4d, in which the GFP–myosin molecules dispersed in about 15 s.

Discussion

The contraction rates of the Triton cytoskeletons are comparable to those in physiological processes

The typical time scales for the changes in the intact cells are expected to be longer than those measured on cytoskeletons on the weakly adhesive substrates, because resistive forces acting in intact cells are larger, in part due to the effect of osmotic pressure. One example studied in a previous work[52] is the apical constriction of cells during the development of *Caenorhabditis elegans* and *Drosophila*. That change is driven by local contraction of the actomyosin cortex, and the time required is of the order of 10 min. Another example is the dynamics of the contractile ring during cytokinesis: a previous study of this process in *Dictyostelium* cells[24] showed that the main part of the process requires a time of the order of minutes, and that the contraction rate (estimated from Fig. 3 in that article using the equation $d\varepsilon/dt = d(\ln D)/dt$, D being the diameter of the equatorial ring) is roughly 0.015 s^{-1} for wt cells. The rate is 0.09 s^{-1} for mutant cells lacking racE or dynacortin since these proteins were found to slow down the contraction process. A comparison with the contraction rate of ~0.04 s^{-1} of wt cytoskeletons suggests that the contractile rings behave nearly like the Triton cytoskeletons, as if the resistive forces exerted by the plasma membrane, resulting from the higher internal pressure (osmotic pressure in physiological conditions), were of relatively low magnitude. This indicates that an important fraction of the total force exerted by the actomyosin cortex is compensated by other factors, presumably the viscoelasticity of the cortex. Thus, the relatively low contribution of the internal (osmotic) pressure could be explained by a sufficiently thick acto-myosin contractile ring, and in fact it is known that the amount of myosin in the contractile ring increases if the dividing cell is challenged by physical compression.[53] A third example is the blebbing of cells: in this case, the protrusion of the cell membrane (bleb) detached from the cytoskeleton expands, being propelled by the contraction of the cortex, which acts as a pump by contraction. It is reasonable to accept that the formation of a bleb, due to the easy expansion of that part of the membrane, reduces considerably the internal (osmotic) pressure, removing thus the impediment for the contraction of other parts of the cell, where the cortex is attached to the membrane. Accordingly, below a critical cortical tension, blebs cannot expand,[26] and in fact myosin-null *Dictyostelium* cells do not bleb.[54] Besides, the duration of the blebbing process induced in *Dictyostelium* cells by quinine is of the order of tens of seconds.[25]

In the last two examples, the contraction of the cytoskeleton takes place at rates comparable to those in our experiments with wt myosin. As argued above, in both cases, it is reasonable to assume that the effect of internal pressure is low because of the thicker cortex in the contractile ring and the drop in pressure during blebbing. Hence, the cytoskeleton would contract in conditions similar to our experiments, in which the effect of internal pressure was negated by removing the cell membrane. Therefore the comparison supports the idea that in the two examples the contraction rates are determined by a balance between the driving force generated by the acto-myosin system and the viscoelasticity of the cortex. In the case of apical constriction during the development of flies and nematodes,[52] some other factors, including osmotic pressure, probably play major roles in slowing the contraction process. In quiescent cells, contractility is balanced by the internal pressure, yielding no apparent deformation.

The density of myosin molecules actively driving the contraction may be alike in all cytoskeletons

The independence of the contraction rate from the myosin content suggests that the density of myosin molecules actively contributing to contraction of the actomyosin network is, at a given time, alike in all cytoskeletons. Bendix *et al.*[36] found that the speed of contraction of gels containing actin, myosin and cross-linker α-actinin grows with the concentration of myosin below a certain concentration threshold, above which the speed saturates, and Yumura observed that only 6% of total cellular myosin was sufficient to induce contraction of Triton

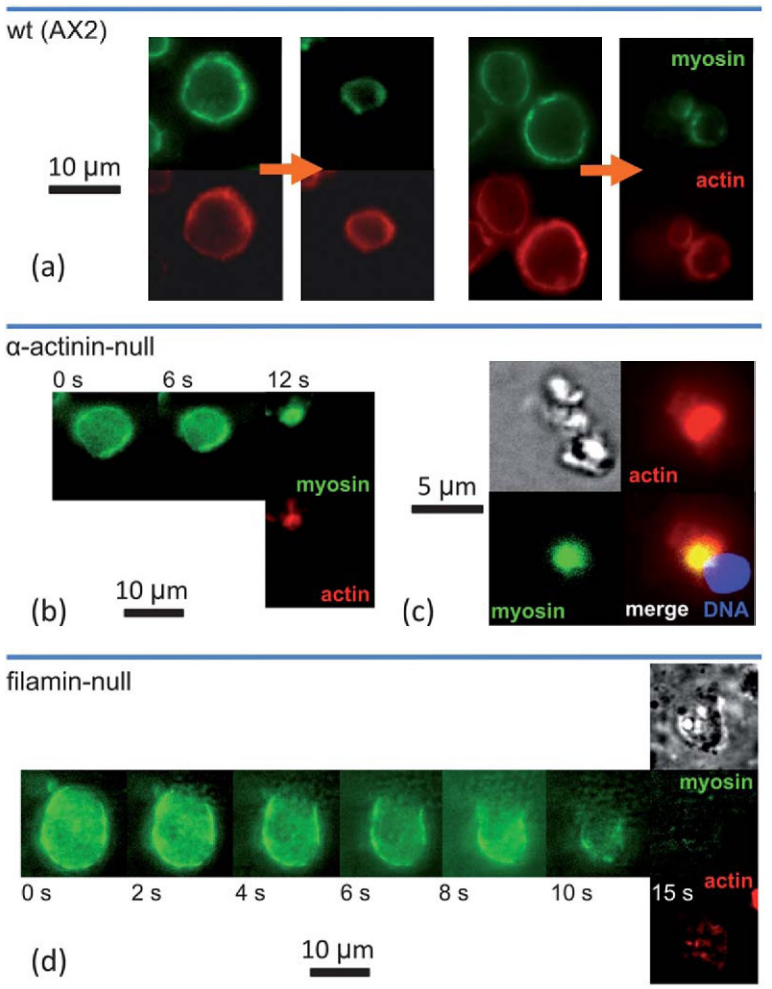

Fig. 4 Fluorescence images showing GFP–myosin and actin (rhodamine phalloidin staining) in the cytoskeletons after the addition of ATP: (a) before and after contraction of wt (AX2) cells, (b) at three different times of the contraction process of an α-actin-null cytoskeleton, and (d) during the disintegration process of a filamin-null cytoskeleton. (c) Contracted cytoskeleton and cellular debris at the end of the process of an α-actin-null cytoskeleton, showing that the nuclear material (Hoechst 33258 staining) has been expelled.

cytoskeletons at the 50% maximum rate.[12] Similarly, in *in vitro* motility assays, the speed of actin filaments saturates over a certain myosin head density on the surface.[55] Therefore, a plausible hypothesis is that the myosin concentration in the Triton cytoskeletons is above an equivalent threshold, and that a large fraction of myosin molecules are not effectively contributing to the contraction process, so that under the present conditions the myosin content is not a limitation for the contraction of the cytoskeletons. It is known that the activity of *Dictyostelium* myosin is inhibited when the regulatory light chain is not phosphorylated,[56] but this mechanism is not involved in inhibiting the activity in the cytoskeletons, since both ΔRLCBS and ΔBLCBS myosins did not bind regulatory light chains and were fully active *in vitro*.[42]

The different contraction rates may be explained by different effects of forces on myosin heads

Previous measurements of the sliding velocity of actin filaments over myosin-coated surfaces *in vitro* without external forces yielded values between 0.6 µm s^{-1} (ΔBLCBS myosin) and 3.0 µm s^{-1} (wt myosin) at 30 °C.[43] At the temperature of the experiments, 22 °C, these values were reduced by 42% for an estimated Arrhenius activation energy of 50 kJ mol^{-1}.[57] Considering a typical length of myosin filaments of 0.5 µm,[41] the corresponding strain rate in the actin network between the extremes of a myosin filament (with sliding heads in both extremes) is 1.4 (ΔBLCBS), 3.7 (ΔRLCBS) and 7.0 s^{-1} (wt) at 22 °C. Any two points of the actin network linked by both extremes of a bipolar myosin filament would approach this rate if the myosin heads as a whole could reach the mentioned sliding velocities. Consequently, this is an estimation of the order of magnitude of the upper limit of the maximum contraction strain rate in a cytoskeleton. The actual strain rate is expected to be lower than this upper limit, but the difference is striking. The contraction strain rates measured in this study were in the range of 0.001 (ΔBLCBS) to 0.04 s^{-1} (wt), thus two to three orders of magnitude smaller than the estimation.

There are two possible and complementary factors obstructing the sliding of myosin heads along actin filaments:

(i) the effect of the resistive forces exerted by the internal materials during the contraction of the network and (ii) the slowing down due to the continuous remodeling of the acto-myosin network, the myosin movement being mostly used in rearrangements of the cytoskeleton and possible local contractions.[58] The term remodeling is used in a general sense, including bending and buckling of the actin filaments (due to their low flexural rigidity[59–61]), the possible redistribution of the cross-links and depolymerization of filaments along which the myosin heads slide. In our experiments, the actin filaments were stabilized by 0.5% polyethylene glycol in the medium[62] and the time required for the contraction of the wt cytoskeletons on a low adhesiveness substrate was of the order of 15 s, *i.e.* it is smaller than the typical turnover period for actin filaments,[63,64] although shorter turnover periods, of the order of seconds, can occur at specific sites within the cell.[65] Therefore, even in physiological conditions, although depolymerization could contribute, it is likely that for such a contraction period the remodeling – at least for a large part of the cytoskeleton – includes essentially redistribution of cross-links and large deformations of actin filaments.

As explained previously, the contraction rate in the cytoskeletons grows with the length of the lever arm of the myosin heads. The adhesiveness of the substrate, due to an interaction between the adsorbed poly-L-lysine molecules and cytoskeletal components, is expected to produce an external resistive load impeding the contraction of the cytoskeletons. In the case of wt myosin and ΔRLCBS myosin in which the length of the lever arm is 8.8 nm and 5.8 nm, respectively, the mean contraction rates were clearly affected by the adhesiveness of the substrate, while the contraction strain rates for ΔBLCBS myosin (with the 1.8 nm lever arm) were similar on the two substrates. The ratio between the contraction rates on the two substrates as a function of the length of the lever arm is presented in Fig. 5a, showing that the effect of the adhesive force is higher for longer lever arms. The influence of lever arm length is in agreement with previous studies on the binding of smooth muscle myosin II to actin filaments by Veigel *et al.*,[66] which showed that the time during which myosin heads are attached to actin in each mechanical cycle grows with the pulling force, *i.e.* the force in the opposite direction to the movement of myosin. The torque applied to the myosin motor domain is given by the pulling force multiplied by the length of the lever arm. Rotation of the lever arm would take place at a rate that decreases exponentially with the torque and such a kinetic effect is explained by the Arrhenius transition state theory.[66] This idea is illustrated in

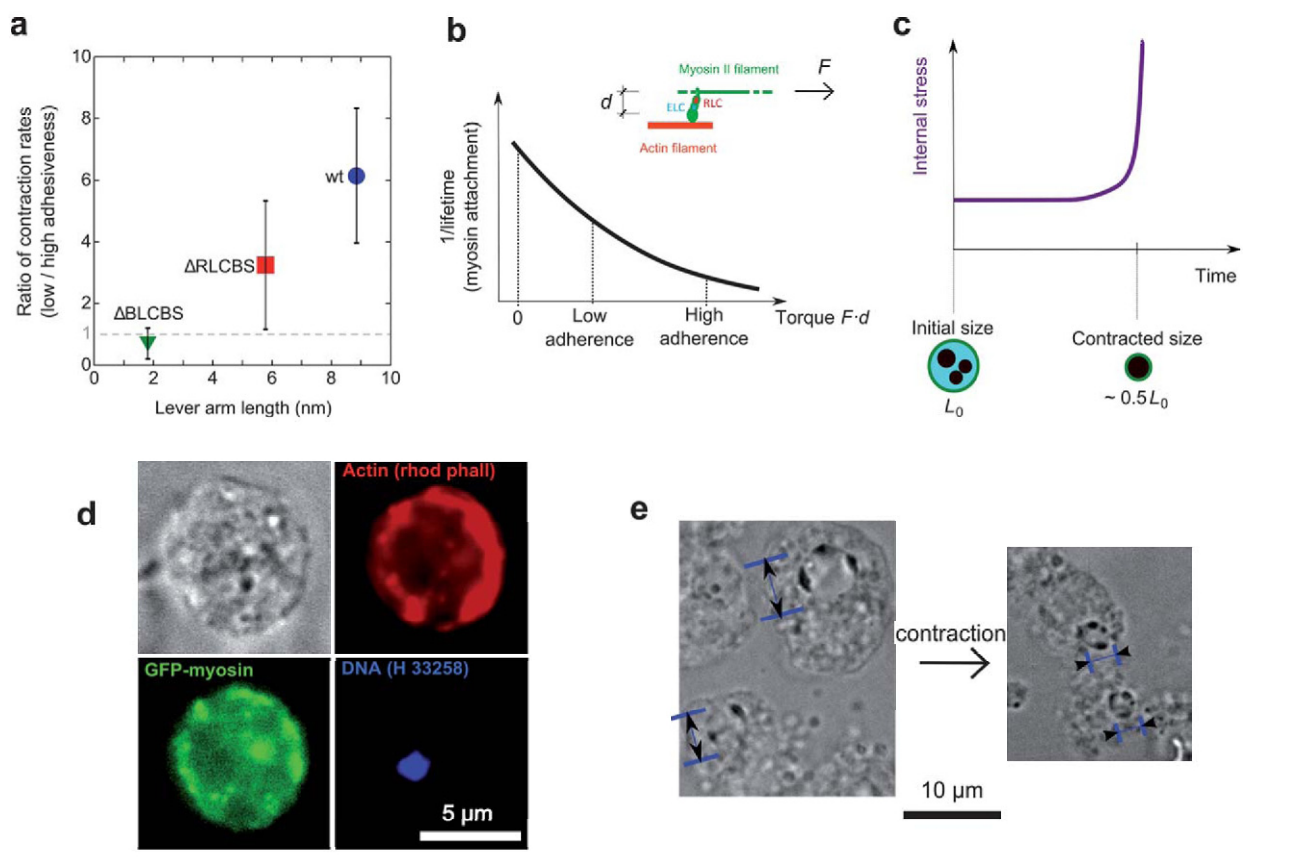

Fig. 5 (a) Ratio between the contraction rate on the low adhesiveness substrates and that on the high adhesiveness substrates. (b) Diagram illustrating the relationship between the torque (product of pulling force F and lever arm distance) in a myosin head and the inverse of the attachment time to actin filaments, based on the work of Veigel *et al.*[66] The duration of the attached state grows exponentially with the pulling torque. (c) Sketch of the proposed change of the internal stress, equal to the mean force per unit area of the internal surface of the cortex. (d) Contracted cytoskeleton with wt myosin observed using a confocal microscope; the fluorescence images show the distribution of GFP–myosin, actin filaments (Rh-Ph staining) and DNA (Hoechst 33258 staining). (e) Representative confocal images showing nuclear sizes before and after contraction of the cytoskeleton. The nuclear size is also indicated in (d).

Fig. 5b. Thus, for the same pulling force, the longer the lever arm is, the higher the torque is and, as a consequence, mutants with a shorter lever arm are less sensitive to changes in the pulling force (as illustrated by the exponential decay in Fig. 5b). The cytoskeletons with wt myosin are therefore the most susceptible to the applied forces.

The abrupt end of the contraction provides insights into the effects of the process

All the cytoskeletons contract to a quite similar minimum size (Fig. 2a), regardless of the myosin type, although one would expect that the stronger myosin (ΔBLCBS) could produce a higher contraction of the internal materials. Moreover, as shown for the three examples in Fig. 1b, even the cytoskeletons with the weakest myosin (wt) maintain a high contraction rate until the abrupt end of the contraction process. These facts indicate that there must be a sudden increase in the resistive forces exerted by the internal materials when the cytoskeletons reach a certain size. These forces are strong enough to stop the contraction process for the three myosins. This change in the mechanical behavior of the material is reasonably identified as the transition from the contracting stage while the cytoplasmic fluid is expelled through the actomyosin cortex to the final contracted state when the forces are resisted by the internal materials (nucleus, debris of other organelles and the cytoskeleton). We confirmed that both the nucleus and the actin filaments are present in the contracted cytoskeletons by fluorescence microscopy, as in the example shown in Fig. 5d. Besides, the final sizes of the compacted nuclei were much smaller than the initial sizes in the confocal images, as illustrated in Fig. 5e.

The proposed scheme for the contraction process is sketched in Fig. 5c. The figure represents schematically the changes in the stress, *i.e.* the mean force per unit area of the internal surface of the cortex. During the progression of contraction, the main effect is to compact the contents and the actomyosin network, expelling the internal fluid. In the final contracted state, most of the free fluid has been expelled.

The cross-linking proteins are key components during the contraction process

The results indicate that the lack of α-actinin yields (i) a higher contraction rate, which could be due to a higher speed of remodeling of the actin network, assuming that remodeling is one key process during the contraction of the cytoskeleton; and (ii) also a lower capacity to retain the internal materials inside the cytoskeleton. The reduced growth rate under osmotic stress, previously described for these mutant cells,[49,50] could be related to the impairment of nutrient uptake, which is dependent on the actomyosin cytoskeleton.

The behavior is very different for filamin-null cytoskeletons. Since ATP allows the myosin filaments to slide along actin filaments, an obvious explanation for the disruption of filamin-null cytoskeletons is that the internal forces produced by the sliding of myosin molecules are high enough to separate the actin filaments if they are not cross-linked by filamin, leading to the destruction of the cytoskeleton in the absence of the plasma membrane. Additionally, myosin filaments may act as cross-linkers themselves and this activity would be weakened when ATP dissociates the actin–myosin crossbridges.

In physiological conditions, the cytoskeleton of filamin-null cells is confined by the membrane, and thus it may be stable and contractile even if the actin filaments may detach from one another at some points by the action of myosin filaments. Indeed, the proteins anchoring actin filaments to the membrane would contribute to provide additional indirect cross-linking points. However, the striking behaviour of the filamin-null Triton cytoskeletons should be reflected in the phenotype of filamin-null cells in some way. As mentioned above, they are viable and the most noticeable difference from wt cells is the defective phototaxis of slugs at the multicellular stage of *Dictyostelium* development. In this sense, it has been suggested that filamin is involved in signaling, which controls the migration process, although the role of this molecule is most likely complex.[50] Our results suggest that the defective performance of filamin-null cells could have originated from the imperfect contraction of the actomyosin cytoskeleton, presumably resulting in a lower cortical tension.

The critical effect of filamin is in agreement with previous studies of reconstituted actin networks,[47] which showed that the filamin cross-linked networks are considerably more resistant to deformation than the α-actinin cross-linked ones in the same conditions. This difference has been attributed to the preferential binding of α-actinin to parallel actin filaments,[47] yielding a low proportion of cross-links between non-parallel filaments. Unlike smooth muscle α-actinin, however, *Dictyostelium* α-actinin cross-links filaments to form networks, rather than bundles, *in vitro*.[48] This activity is similar to that of filamin and, therefore, we are not certain whether the apparent differences in the behaviours of α-actinin-null and filamin-null cytoskeletons represent qualitative differences in their activities or simply a quantitative difference such that filamin is the major cross-linker in *Dictyostelium* and loss of α-actinin produces less severe defects, *i.e.* faster contraction without disintegration.

Experimental

Strains

We used the mutant *Dictyostelium discoideum* cell line HS1 (ref. 67) that lacks the endogenous myosin heavy chain gene. The cells were maintained on plastic Petri dishes in HL5 medium[68] containing additional 60 μg each of penicillin and streptomycin per ml (thus named HL5PS) at 22 °C. The cells were transfected with pTIKL (extrachromosomal vector with a G418-resistance gene) carrying either one of the mutant or wt myosin heavy chain genes that were fused N-terminally with the S65T mutant GFP gene. Transfected cells were selected and maintained in HL5PS medium in the presence of 12 μg ml^{-1} G418 (Invitrogen, Tokyo, Japan). The three different types of myosin heavy chain are (a) wt, (b) mutant myosin with an internal deletion that removes the regulatory light chain binding site, ΔRLCBS,[42] and (c) a mutant lacking both light chain binding sites, ΔBLCBS.[43]

To study the influence of actin binding proteins, we used mutant *D. discoideum* strains lacking α-actinin or filamin generated and described in previous studies.[49,69] These strains were obtained from the Dicty Stock Center, and their IDs were DBS0235459 and DBS0236077, respectively. AX2 is an axenically growing parent strain of these two mutants, and was tested as the wt reference. The cells were maintained in HL5PS medium. To allow observation of the myosin molecules by fluorescence microscopy, the cells were transfected with pDdBsr (extrachromosomal vector with a blasticidin-resistance gene[21]) carrying the GFP-fused wt myosin heavy chain gene described above. Transfected cells were selected and maintained in HL5PS medium with 6 μg ml^{-1} blasticidin S (Funakoshi, Tokyo, Japan).

Experiments of contraction of Triton cytoskeletons

The contraction experiments were carried out on plastic glass-bottomed Petri dishes with a diameter of 35 mm (Iwaki Glass, Tokyo, Japan). Before use, the dishes were incubated for 1 h with 0.0001% or 0.0010% (w/v) poly-L-lysine (M_w = 150–300 kDa, Sigma, St. Louis, MO, USA) solutions. These dishes are called weak and high adhesiveness substrates, respectively. The plates were thoroughly rinsed with water and cells in HL5 medium were allowed to settle on them. After 30 min, the medium was replaced by a low-fluorescent medium (H. MacWilliams, http://dictybase.org) and the cells were maintained there for at least 30 min. This second medium was replaced by 1 ml of lysis buffer with composition based on a previous study by Yumura:[12] 15 mM KCl, 2 mM $MgCl_2$, 5 mM EGTA, 1 mM DTT, 0.2 mM PMSF, 0.5% polyethylene glycol (M_r = 4000; Wako Pure Chemicals, Osaka, Japan), 0.1% NaN_3, 10 mM benzamidine, and 10 mM HEPES (pH 7.5). The plate was immediately placed on a phase contrast/fluorescent microscope (IX-71, Olympus, Tokyo, Japan) equipped with a 100× UPlanApo objective (NA = 1.35), and 1 ml of lysis buffer containing 0.4% Triton X-100 was added. After approximately 6 min, 1 ml of lysis buffer with 2 mM ATP was added. The nominal temperature was 22 °C.

Time lapse GFP fluorescence images of contracting Triton-ghosts were acquired by using the IP LAB software package (Scanalytics, Billerica, MA, USA). Phase contrast images were obtained before the addition of each component and at the end of the experiment. In some experiments, after the contraction was complete, the nucleus and the actin filaments were respectively visualized by incubation with 0.6 μg ml^{-1} Hoechst 33258 and 20 nM rhodamine phalloidin for 10 min.

Digital analysis

The micrographs were analyzed with Image J software (http://rsb.info.nih.gov/ij). For each studied cell, the total cross-section area, A, and the mean intensity were measured in each fluorescence micrograph (Fig. 1a). The nominal size of the cell, L, was calculated as the diameter of an equivalent circular section, $L = (4A/\pi)^{1/2}$. True strain was obtained as $\varepsilon = \ln(L/L_0)$, L_0 being the initial nominal size. The mean fluorescence intensity was corrected by subtracting the mean intensity of the background.

In total, 180 cytoskeletons were studied by digital analysis, measuring their initial and final characteristics; 100 were completely analyzed, obtaining the relationship between true strain ε and time t. The maximum contraction strain rate was calculated as the maximum value of $-d\varepsilon/dt$, computing $d\varepsilon/dt$ by linear fitting of the curve ε *vs.* t for a period of at least 10 s. For this magnitude, the number of measurements was 28, 14 and 14 at low adhesiveness and 11, 10 and 23 at high adhesiveness for wt, ΔRLCBS and ΔBLCBS myosins, respectively.

Conclusion

The procedure described in this work, based on the use of adhesive substrates and fluorescence imaging, allows the contraction of actomyosin cytoskeletons to be studied. During contraction, the internal materials are compacted by expelling the cytoplasmic fluid. The actin network undergoes large deformations, presumably involving remodeling by redistribution of the cross-linking molecules. The importance of the cross-links is substantiated by the results of mutants lacking α-actinin, since the contraction rate is higher in the absence of the cross-linker. The cytoskeletons remained contracted after a reduction in GFP-content by diffusion, indicating that they had suffered plastic deformation. The rate depends on the sliding velocity of the myosin heads, but it is two orders of magnitude slower than that predicted by the sliding velocity of purified actin–myosin movements *in vitro*, presumably due to the resistive force exerted by viscoelastic properties of the cortex, internal materials and the substrate. Robinson and Zhang[24] calculated that the contraction speed of intact contractile rings is also two orders of magnitude slower than that predicted from the *in vitro* velocity of actin–myosin movements; moreover, the contraction rate of cytoskeletons on less adhesive substrates is between the contraction rates of wt and the faster mutant contractile rings. This comparison suggests that osmotic pressure, which is impeding the contraction of intact contractile rings but not isolated cytoskeletons, plays a relatively minor role in determining the contraction rates of contractile rings, showing the usefulness of the experimental system reported here to elucidate how contraction rates of intact cells are determined.

The two cross-linking proteins studied affect dramatically the behavior of contractile cytoskeletons. The presence of α-actinin reduces the contraction rate while filamin is required to maintain the integrity of the cytoskeleton during contraction. These results allow us to envisage this technique as a promising method to study the role of the whole ensemble of cytoskeleton components.

Acknowledgements

The authors thank Dr Akira Nagasaki for his kind help in microscopy, and the Dicty Stock Center and Japan National Bioresource Project Cellular Slime Molds (NBRP-Nenkin) for providing us with the actinin-null and filamin-null mutant cell lines. GRP received a grant for a short stay abroad from Fundación Caja de Madrid. This work was supported in part by grants-in-aid for scientific research from the Ministry of Education, Culture, Sports, Science and Technology of Japan (to TU).

References and notes

1 D. A. Fletcher and R. D. Mullins, *Nature*, 2010, **463**, 485–492.
2 T. D. Pollard and G. G. Borisy, *Cell*, 2003, **112**, 453–465.
3 A. L. Hitt and E. J. Luna, *Curr. Opin. Cell Biol.*, 1994, **6**, 120–130.
4 A. Bretscher, *Annu. Rev. Cell Biol.*, 1991, **7**, 337–374.
5 V. Niggli and M. M. Burger, *J. Membr. Biol.*, 1987, **100**, 97–121.
6 M. Clarke and J. A. Spudich, *J. Mol. Biol.*, 1974, **86**, 209–222.
7 J. S. Davis, *Annu. Rev. Biophys. Biophys. Chem.*, 1988, **17**, 217–239.
8 S. Yumura and T. Kitanishi-Yumura, *Cell Struct. Funct.*, 1990, **15**, 343–354.
9 S. S. Margossian and S. Lowey, *Biochemistry*, 1978, **17**, 5431–5439.
10 Y. Y. Toyoshima, S. J. Kron, E. M. McNally, K. R. Niebling, C. Toyoshima and J. A. Spudich, *Nature*, 1987, **328**, 536–539.
11 E. R. Kuczmarski, L. Palivos, C. Aguado and Z. L. Yao, *J. Cell Biol.*, 1991, **114**, 1191–1199.
12 S. Yumura, *Cell Struct. Funct.*, 1991, **16**, 481–488.
13 D. Wessels, D. R. Soll, D. Knecht, W. F. Loomis, A. De Lozanne and J. Spudich, *Dev. Biol.*, 1988, **128**, 164–177.
14 M. Tsujioka, S. Yumura, K. Inouye, H. Patel, M. Ueda and S. Yonemura, *Proc. Natl. Acad. Sci. U. S. A.*, 2012, **109**, 12992–12997.
15 I. Mabuchi and M. Okuno, *J. Cell Biol.*, 1977, **74**, 251–263.
16 D. A. Knecht and W. F. Loomis, *Science*, 1987, **236**, 1081–1086.
17 A. De Lozanne and J. A. Spudich, *Science*, 1987, **236**, 1086–1091.
18 S. L. Moores, J. H. Sabry and J. A. Spudich, *Proc. Natl. Acad. Sci. U. S. A.*, 1996, **93**, 443–446.
19 T. Q. P. Uyeda and S. Yumura, *Micro. Res. Tech.*, 2000, **49**, 136–144.
20 G. R. Plaza, *Phys. Rev. E: Stat., Nonlinear, Soft Matter Phys.*, 2010, **82**, 031902.
21 T. Q. P. Uyeda, Y. Iwadate, N. Umeki, A. Nagasaki and S. Yumura, *PLoS One*, 2011, **6**, e26200.
22 K. Hayakawa, H. Tatsumi and M. Sokabe, *J. Cell Biol.*, 2011, **195**, 721–727.
23 V. I. Risca, E. B. Wang, O. Chaudhuri, J. J. Chia, P. L. Geissler and D. A. Fletcher, *Proc. Natl. Acad. Sci. U. S. A.*, 2012, **109**, 2913–2918.
24 W. Zhang and D. N. Robinson, *Proc. Natl. Acad. Sci. U. S. A.*, 2005, **102**, 7186–7191.
25 K. Yoshida and K. Inouye, *J. Cell Sci.*, 2001, **114**, 2155–2165.
26 J. Y. Tinevez, U. Schulze, G. Salbreux, J. Roensch, J. F. Joanny and E. Paluch, *Proc. Natl. Acad. Sci. U. S. A.*, 2009, **106**, 18581–18586.
27 A. J. Ridley, *Cell*, 2011, **145**, 1012–1022.
28 A. Zumdieck, K. Kruse, H. Bringmann, A. A. Hyman and F. Jülicher, *PLoS One*, 2007, **2**, e696.
29 T. D. Pollard, *Curr. Opin. Cell Biol.*, 2010, **22**, 50–56.
30 G. Salbreux, G. Charras and E. Paluch, *Trends Cell Biol.*, 2012, **22**, 536–545.
31 M. P. Stewart, J. Helenius, Y. Toyoda, S. P. Ramanathan, D. J. Muller and A. A. Hyman, *Nature*, 2011, **469**, 226–230.
32 Y. Fukui, A. De Lozanne and J. A. Spudich, *J. Cell Biol.*, 1990, **110**, 367–378.
33 J. C. Effler, P. A. Iglesias and D. N. Robinson, *Cell Cycle*, 2007, **6**, 30–35.
34 R. Merkel, R. Simson, D. A. Simson, M. Hohenadl, A. Boulbitch, E. Wallraff and E. Sackmann, *Biophys. J.*, 2000, **79**, 707–719.
35 M. K. Pramanik, M. Iijima, Y. Iwadate and S. Yumura, *Genes Cells*, 2009, **14**, 821–834.
36 P. M. Bendix, G. H. Koenderink, D. Cuvelier, Z. Dogic, B. N. Koeleman, W. M. Brieher, C. M. Field, L. Mahadevan and D. a. Weitz, *Biophys. J.*, 2008, **94**, 3126–3136.
37 J. S. Condeelis and D. L. Taylor, *J. Cell Biol.*, 1977, **74**, 901–927.
38 H. Strzelecka-Gołaszewska, U. Piwowar and B. Pliszka, *Eur. J. Cell Biol.*, 1981, **24**, 116–123.
39 D. Mizuno, C. Tardin, C. F. Schmidt and F. C. Mackintosh, *Science*, 2007, **315**, 370–373.
40 M. Soares e Silva, M. Depken, B. Stuhrmann, M. Korsten, F. C. MacKintosh and G. H. Koenderink, *Proc. Natl. Acad. Sci. U. S. A.*, 2011, **108**, 9408–9413.
41 S. Yumura and Y. Fukui, *Nature*, 1985, **314**, 194–196.
42 T. Q. P. Uyeda and J. A. Spudich, *Science*, 1993, **262**, 1867–1870.
43 T. Q. P. Uyeda, P. D. Abramson and J. A. Spudich, *Proc. Natl. Acad. Sci. U. S. A.*, 1996, **93**, 4459–4464.
44 M. A. Meyers and K. K. Chawla, *Mechanical Behavior of Materials*, Cambridge University Press, Cambridge, UK, 2nd edn, 2008.
45 J. Zang, G. Cavet, J. H. Sabry, P. Wagner, S. L. Moores and J. A. Spudich, *Mol. Biol. Cell*, 1997, **8**, 2617–2629.
46 E. Ponte, F. Rivero, M. Fechheimer, A. Noegel and S. Bozzaro, *Mech. Dev.*, 2000, **91**, 153–161.
47 M. L. Gardel, F. Nakamura, J. H. Hartwig, J. C. Crocker, T. P. Stossel and D. A. Weitz, *Proc. Natl. Acad. Sci. U. S. A.*, 2006, **103**, 1762–1767.
48 D. S. Courson and R. S. Rock, *J. Biol. Chem.*, 2010, **285**, 26350–26357.
49 F. Rivero, R. Furukawa, M. Fechheimer and A. A. Noegel, *J. Cell Sci.*, 1999, **112**, 2737–2751.
50 N. Khaire, R. Müller, R. Blauwasser, L. Eichinger, M. Schleicher, M. Rief, T. A. Holak and A. A. Noegel, *J. Biol. Chem.*, 2007, **282**, 1948–1955.
51 S. L. Blagg, S. E. Battom, S. J. Annesley, T. Keller, K. Parkinson, J. M. F. Wu, P. R. Fisher and C. R. L. Thompson, *Development*, 2011, **138**, 1583–1593.
52 M. Roh-Johnson, G. Shemer, C. D. Higgins, J. H. McClellan, A. D. Werts, U. S. Tulu, L. Gao, E. Betzig, D. P. Kiehart and B. Goldstein, *Science*, 2012, **335**, 1232–1235.
53 R. Neujahr, C. Heizer, R. Albrecht, M. Ecke, J. M. Schwartz, I. Weber and G. Gerisch, *J. Cell Biol.*, 1997, **139**, 1793–1804.
54 K. Yoshida and T. Soldati, *J. Cell Sci.*, 2006, **119**, 3833–3844.
55 T. Q. P. Uyeda, S. J. Kron and J. A. Spudich, *J. Mol. Biol.*, 1990, **214**, 699–710.
56 L. M. Griffith, S. M. Downs and J. A. Spudich, *J. Cell Biol.*, 1987, **104**, 1309–1323.
57 M. Anson, *J. Mol. Biol.*, 1992, **224**, 1029–1038.

58 S. Yumura and T. Kitanishi-Yumura, *J. Cell Biol.*, 1992, **117**, 1231–1239.
59 F. Gittes, B. Mickey, J. Nettleton and J. Howard, *J. Cell Biol.*, 1993, **120**, 923–934.
60 M. Vicente-Manzanares, X. Ma, R. S. Adelstein and A. R. Horwitz, *Nat. Rev. Mol. Cell Biol.*, 2009, **10**, 778–790.
61 M. J. Footer, J. W. J. Kerssemakers, J. A. Theriot and M. Dogterom, *Proc. Natl. Acad. Sci. U. S. A.*, 2007, **104**, 2181–2186.
62 J. Goverman, L. A. Schick and J. Newman, *Biophys. J.*, 1996, **71**, 1485–1492.
63 H. Y. Kueh, W. M. Brieher and T. J. Mitchison, *Proc. Natl. Acad. Sci. U. S. A.*, 2008, **105**, 16531–16536.
64 D. N. Robinson, S. S. Ocon, R. S. Rock and J. A. Spudich, *J. Biol. Chem.*, 2002, **277**, 9088–9095.
65 S. Yumura, G. Itoh, Y. Kikuta, T. Kikuchi, T. Kitanishi-Yumura and M. Tsujioka, *M. Biol. Open*, 2013, **2**, 200–209.
66 C. Veigel, J. E. Molloy, S. Schmitz and J. Kendrick-Jones, *Nat. Cell Biol.*, 2003, **5**, 980–986.
67 K. M. Ruppel, T. Q. P. Uyeda and J. A. Spudich, *J. Biol. Chem.*, 1994, **269**, 18773–18780.
68 M. Sussman, *Methods Cell Biol.*, 1987, **28**, 9–29.
69 L. Eichinger, B. Köppel, A. A. Noegel, M. Schleicher, M. Schliwa, K. Weijer, W. Witke and P. A. Janmey, *Biophys. J.*, 1996, **70**, 1054–1060.